International Journal on Magnetic Particle Imaging
Vol 9, No 1, Suppl 1, Article ID 2303032, 4 Pages

Proceedings Article

First Human Brain-Scale Magnetic Particle Imaging System with Superconductor

Tuan-Anh Le[a,b] · Minh Phu Bui[a] · Khaled Mohamed Gadelmowla[c] · Seungjun Oh[a] · Jungwon Yoon[a,*]

[a]School of Integrated Technology, Gwangju Institute of Science and Technology, Gwangju 61005, Republic of Korea
[b]Department of Physiology and Biomedical Engineering, Mayo Clinic, Scottsdale, Arizona 85259, USA
[c]Energy Science, Sungkyungwan University, Suwon 16419, South Korea
[*]Corresponding author, email: jyoon@gist.ac.kr

Abstract

Magnetic particle imaging (MPI) is an emerging non-invasive medical imaging method that can determine the concentration and location of superparamagnetic iron oxide (SPIO) nanoparticles. However, the scalability of magnetic particle imaging (MPI) is, currently, the major barrier to its clinical use. For a human bore size MPI, it is important to achieve a high magnetic gradient to obtain high image resolution with a sufficiently large field-of-view (FOV). In this paper, we present a human brain-scale amplitude modulation (AM) MPI system with a bore size of 200 mm. By using superconductor coils, the proposed MPI system can reach a high magnetic field gradient up to 2.5 T/m/µ0 and a 1D-FOV of 97.6 mm (a feasible 3D FOV of 148.8 × 137.6 × 97.6 mm^3). These promising results show that the scalability of MPI for human application is not far away.

I. Introduction

MPI is a new medical imaging method that can determine the concentration and position of superparamagnetic iron oxide (SPIO) nanoparticles [1]. MPI enables high-resolution, high-sensitivity, and real-time imaging without non-ionizing radiation that is suitable for most medical applications. Therefore, MPI has been deployed for several applications such as vascular and perfusion imaging, oncology imaging, cell tracking, inflammation imaging, trauma imaging [2, 3], navigation for magnetic drug delivery [4-9], and magnetic hyperthermia [10-12]. Because of the challenges in its scalability, there are very few human-scale MPI systems [13-16] at the moment. The concept of a whole-body MPI system for human application was first presented by Philips [13]. In 2015, Philips withdrew from MPI development due to economic reasons. In 2017, Mason et al. [14] designed a functional brain scanner and demonstrated the feasibility of MPI for human brain application. In 2019, a real MPI scanner for human brain application was presented [15]. In 2022, Vogel et al. [16] proposed a human-sized MPI scanner based on the Traveling Wave approach [17]. However, almost all current human-scale MPI systems have relatively small gradients (up to ~0.7 T/m/μ_0) with a low spatial resolution that is not sufficient for most human applications. Due to the limitations of existing nanoparticle tracers and reconstruction methods, a human MPI scanner would need a gradient field with an high field gradient of 2 T/m/μ_0 to provide an acceptable spatial resolution [18], while retaining a FOV with a minimum space of 200 mm to position the patient [13, 19]. Although using softcore is a feasible approach to design a human scanner with magnetic field gradients up to 2.5-3

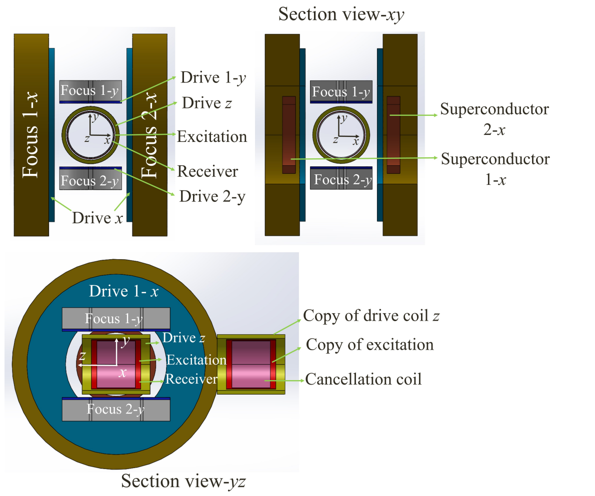

Figure 1: Coil topologies of the proposed MPI system.

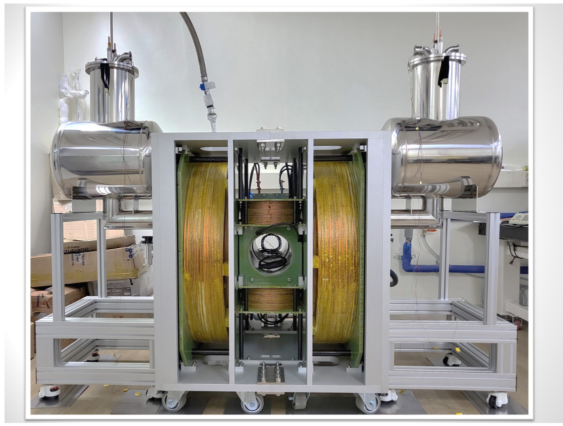

Figure 2: Final system of the human brain-scale AM MPI system.

T/m/μ_0 [8, 19], the size, weight, and power consumption of the system will increase significantly due to the limitations related to the magnetization characteristic of the softcore and its space occupation. A superconductor coil is one of the best solution to reduce the size and the power requirement for the system with the capacity of magnetic field gradients up to 6 T/m/μ_0 in a human-scale MPI scanner [20].

In this paper, we developed a human-scale AM MPI system with superconductor selection coils, which can achieve high field gradient up to 2.5 T/m/μ_0, 1D FOV of 100 mm at 2.5 T/m/μ_0 with possible 3D FOV of 148.8 $\times$137.6 $\times$ 97.6 mm^3, and a bore size of 200 mm. However, its total size and maximum power requirement (about 70 kW) is similar to the rabbit-scale AM MPI system [21].

II. Coil concept

The coil setup for the proposed MPI system using superconductor coils is shown in Figure 1. The system has eight parts (superconductor selection, drive [drive coils *x*, *y*, and *z*], focus [focus coils *x*, *y*], excitation, receiver, copy of drive-*z*, copy of the excitation, and cancellation coils).

The superconductor selection coils in Maxwell configuration were used to produce a movable field-free point (FFP) along the *x*-axis. To minimizing the size of the system, the superconductor part was arranged inside the focus coil *x*. The drive fields along the *x*-, y-, and *z*-axes, with high-amplitudes and low-frequencies ($\leq$ 400 Hz), were used to scan FFP for creating a partial FOV (pFOV). To generate the drive fields in the *x*, *y*, and *z*-axes, cylinder-shaped coils (drive coil *z*) and coils with Helmholtz configurations (drive coils *x* and *y*) were used. Although the AM method can use a high magnetic field to generate a whole FOV (wFOV) with human-scale size, focus field should be used to reduce the amplitude of the drive fields. This can avoid the effect of AC fields of drive fields coupling into the superconductor coils. The superconductor coils were cooled by using cryo-chambers filled by liquid Helium. The cryo-chamber outer was used as a shielding that also help reducing the effect of other fields coupling into the superconductor coils.

To create the focus fields in the *x*, y-axes, coils with Helmholtz configurations (focus coils *x* and *y*) were used. In this system, the patient can be moved in z-axis to change the pFOV or wFOV, focus coils on *z*-direction were not added to minimize the complexity of the system. The excitation field of the excitation coil along the *z*-axis (collinear with the bore) was used to excite the magnetization of the particles and generate the signal. To measure the particles' signal, a cylindrical receiver coil collinear with the bore was used. To prevent the drive field *z* and excitation field feed-through signals and match the range of particles' signal with the analog digital converter (ADC), copy of the drive coil *z*, copy of the excitation coil, and the cancellation coil collinear with the bore were used for the cancellation method [7, 21] (Since the FFP trajectory was along the *z*-direction, the feed-through from the drive *x* and y were small and can be ignored). In this system, the water-cooling system was used for all coils except for the superconductor part, excitation, receiver, and cancellation coils.

III. Results

A photograph of the proposed MPI system is shown in Figure 2. Coil parameters and system parameters of the MPI scanner are provided in Table 1 and Table 2, respectively.

Figure 3 shows the detail connection diagram of the human-scale MPI scanner.

The system can achieve a high gradient field up to 2.5

10.18416/ijmpi.2023.2303032

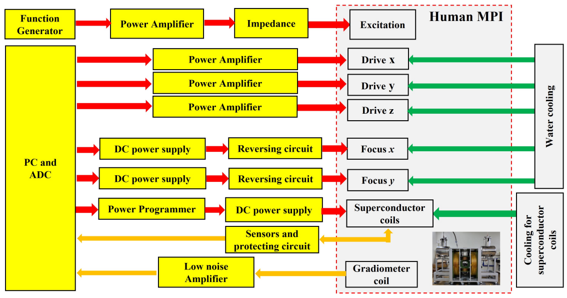

Figure 3: Connection diagram for the human brain-scale MPI scanner.

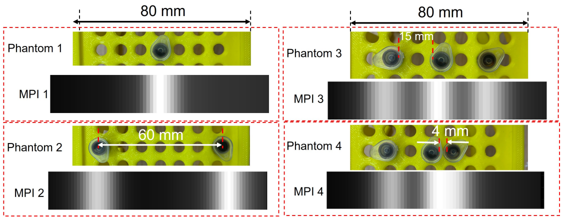

Figure 4: 1D MPI results with $G_x = 2.5$ T/m/μ_0, $G_z = 1.25$ $T/m/\mu_0$. The phantoms were positioned along the z-axis. The phantom size is 80 mm and wFOV = 97.6 mm.

Table 1: Coil parameters

Names	Turns	Size information (mm)	Wire information
Selection coils	2220	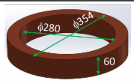	0.78 (mm^2)
Focus x	864	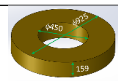	22.57 (mm^2)
Focus y	414	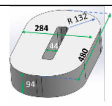	16.36 (mm^2)
Drive x	104	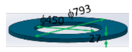	22.57 (mm^2)
Drive y	46	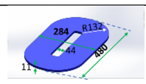	16.36 (mm^2)
Drive z or copy	160	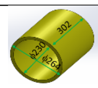	29.69 (mm^2)
Excitation or copy	72	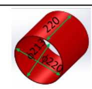	Litz wire 1500/36 AWG
Receiver or cancellation	244	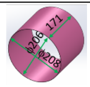	Litz wire 140/46 AWG

T/m/μ_0 with a bore size of 200 mm and possible wFOV 148.8 ×137.6 × 97.6 mm^3 at 2.5 T/m/μ_0, while maintaining a similar total size and power requirement (about 70 kW) to the rabbit-scale AM MPI [21].

As shown in Figure 4, 1D MPI results were obtained to demonstrate the proposed system's performance. Here, the AM reconstruction method [21] was used to acquire MPI images. The phantom used in the experiments consisted of one, two, and three SPIOs spots. Each spot consisted of 50 µL Resovist particles (Meito Sangyo Co. Ltd., Nagoya, Japan). The system was able to achieve a 1D wFOV of 97.6 mm at $G_x = 2.5$ T/m/μ_0. Therefore, combining MPI with a superconductor technology can lead to a high magnetic field gradient that might facilitate human application of MPI soon.

IV. Conclusions

Using AM MPI, we could overcome the scalability issues of the general MPI systems and for the first time enabling the utilization of superconductor technology in human-scale MPI systems. The proposed MPI system reached a 1D wFOV of 97.6 mm at 2.5 T/m/μ_0. 3D MPI imaging tests of SPIOs should be performed to verify the performance of the proposed design in future works.

Author's statement

Research funding: This work was supported in part by the National Research Foundation of Korea under Grant 2019M3C1B8090798, in part by the Korea Evaluation Institute of Industrial Technology under Grant 20003822, and in part by the Korea Medical Device Development under Grant 202012E12. Conflict of interest: Authors state no conflict of interest.

References

[1] B. Gleich and J. Weizenecker, "Tomographic imaging using the nonlinear response of magnetic particles," Nature, vol. 435, no. 7046, pp. 1214-1217, 2005.

[2] L. Wu et al., "A review of magnetic particle imaging and perspectives on neuroimaging," American Journal of Neuroradiology, vol. 40, no. 2, pp. 206-212, 2019.

[3] T. Knopp, N. Gdaniec, and M. Möddel, "Magnetic particle imaging: from proof of principle to preclinical applications," Physics in Medicine & Biology, vol. 62, no. 14, p. R124, 2017.

[4] M. P. Bui, T.-A. Le, and J. Yoon, "A Magnetic Particle Imaging-based Navigation Platform for Magnetic Nanoparticles using Interactive Manipulation of a Virtual Field Free Point to Ensure Targeted Drug Delivery," IEEE Transactions on Industrial Electronics, 2020.

[5] T.-A. Le, X. Zhang, A. K. Hoshiar, and J. Yoon, "An electromagnetic navigation system with real-time 2D magnetic particle imaging for targeted drug delivery," in 2017 IEEE/RSJ International Conference on Intelligent Robots and Systems (IROS), 2017, pp. 1895-1900: IEEE.

10.18416/ijmpi.2023.2303032

Table 2: System parameters

Category	Parameters	Experiment results
Maximum magnetic gradient	$G_x/G_y/G_z$ (T/m/μ$_0$)	~2.5/-1.25/-1.25
Maximum drive field x	H_{Dx0}/f_x	~38 mT /2 Hz
Maximum drive field y	H_{Dy0}/f_z	~18 mT /20 Hz
Maximum drive field z	H_{Dz0}/f_z	~61 mT/ 400 Hz
Maximum focus field x	H_{Fx0}/f_{Fx}	~148 mT /0.1 Hz
Maximum focus field y	H_{Fy0}/f_y	~68 mT /0.1 Hz
Maximum excitation field	H_{E0}/f_e	~2.1 mT / 18.4 kHz

[6] X. Zhang, T.-A. Le, and J. Yoon, "Development of a magnetic nanoparticles guidance system for interleaved actuation and MPI-based monitoring," in 2016 IEEE/RSJ International Conference on Intelligent Robots and Systems (IROS), 2016, pp. 5279-5284: IEEE.

[7] F. Griese et al., "Simultaneous Magnetic Particle Imaging and Navigation of large superparamagnetic nanoparticles in bifurcation flow experiments," Journal of Magnetism and Magnetic Materials, vol. 498, p. 166206, 2020.

[8] X. Zhang, T.-A. Le, A. K. Hoshiar, and J. Yoon, "A soft magnetic core can enhance navigation performance of magnetic nanoparticles in targeted drug delivery," IEEE/ASME Transactions on Mechatronics, vol. 23, no. 4, pp. 1573-1584, 2018.

[9] J. Rahmer, D. Wirtz, C. Bontus, J. Borgert, and B. Gleich, "Interactive magnetic catheter steering with 3-D real-time feedback using multi-color magnetic particle imaging," IEEE transactions on medical imaging, vol. 36, no. 7, pp. 1449-1456, 2017.

[10] P. Chandrasekharan et al., "Using magnetic particle imaging systems to localize and guide magnetic hyperthermia treatment: tracers, hardware, and future medical applications," Theranostics, vol. 10, no. 7, p. 2965, 2020.

[11] Y. Lu et al., "Combining magnetic particle imaging and magnetic fluid hyperthermia for localized and image-guided treatment," International Journal of Hyperthermia, vol. 37, no. 3, pp. 141-154, 2020.

[12] Z. W. Tay et al., "Magnetic particle imaging-guided heating in vivo using gradient fields for arbitrary localization of magnetic hyperthermia therapy," ACS nano, vol. 12, no. 4, pp. 3699-3713, 2018.

[13] I. Schmale, B. Gleich, O. Mende, and J. Borgert, "On the design of human-size MPI drive-field generators using RF Litz wires," in 2015 5th International Workshop on Magnetic Particle Imaging (IWMPI), 2015, pp. 1-1: IEEE.

[14] E. E. Mason, C. Z. Cooley, S. F. Cauley, M. A. Griswold, S. M. Conolly, and L. L. Wald, "Design analysis of an MPI human functional brain scanner," International journal on magnetic particle imaging, vol. 3, no. 1, 2017.

[15] M. Gräser et al., "Human-sized magnetic particle imaging for brain applications," Nature communications, vol. 10, no. 1, pp. 1-9, 2019.

[16] P. Vogel et al., "iMPI–interventional Magnetic Particle Imaging," International Journal on Magnetic Particle Imaging, vol. 8, no. 1 Suppl 1, 2022.

[17] P. Vogel, M. A. Rückert, P. Klauer, W. H. Kullmann, P. M. Jakob, and V. C. Behr, "Traveling wave magnetic particle imaging," IEEE transactions on medical imaging, vol. 33, no. 2, pp. 400-407, 2013.

[18] S. B. Trisnanto and Y. Takemura, "High-frequency Néel relaxation response for submillimeter magnetic particle imaging under low field gradient," Physical Review Applied, vol. 14, no. 6, p. 064065, 2020.

[19] C. Bontus, B. Gleich, B. David, O. Mende, and J. Borgert, "Concept of a Generator for the Selection and Focus Field of a Clinical MPI Scanner," IEEE Transactions on Magnetics, vol. 51, no. 2, pp. 1-4, 2015.

[20] T. Knopp and T. M. Buzug, Magnetic particle imaging: an introduction to imaging principles and scanner instrumentation. Springer Science & Business Media, 2012.

[21] T.-A. Le, M. P. Bui, and J. Yoon, "Development of Small Rabbit-scale Three-dimensional Magnetic Particle Imaging System with Amplitude Modulation Based Reconstruction," IEEE Transactions on Industrial Electronics, 2022.

10.18416/ijmpi.2023.2303032